Optical properties of developing pip and stone fruit reveal underlying structural changes

Birgit Seifert[a], Manuela Zude[a,b,*], Lorenzo Spinelli[c] and Alessandro Torricelli[d]

[a]Leibniz Institute for Agricultural Engineering Potsdam-Bornim, Max-Eyth-Allee 100, 14469 Potsdam, Germany

[b]Beuth University of Applied Sciences Berlin, Luxemburger Straße 10, 13353 Berlin, Germany

[c]Instituto di Fotonica e Nanotecnologie, CNR, piazza L. da Vinci 32, 20133 Milan, Italy

[d]Politecnico di Milano, Dipartimento di Fisica, piazza L. da Vinci 32, 20133 Milan, Italy

*Corresponding author, e-mail: mzude@atb-potsdam.de

Analyzing the optical properties of fruits represents a powerful approach for non-destructive observations of fruit development. With classical spectroscopy in the visible and near-infrared wavelength ranges, the apparent attenuation of light results from its absorption or scattering. In horticultural applications, frequently the normalized difference vegetation index (NDVI) is employed to reduce the effects of varying scattering properties on the apparent signal. However, this simple approach appears limited. In the laboratory, with time-resolved spectroscopy, the absorption coefficient, μ_a, and the reduced scattering coefficient, μ_s', can be analyzed separately. In the present study, these differentiated optical properties were recorded (540–940 nm), probing fruit tissue from the skin up to 2 cm depth in apple (*Malus x domestica* 'Elstar') and plum (*Prunus domestica* 'Tophit plus') harvested four times (65 to 145 days after full bloom). The μ_a spectra showed typical peak at 670 nm of the chlorophyll absorption. The μ_s' at 670 nm in apple changed by 14.7% (18.2 to 15.5 cm^{-1}), while in plum differences of 41.5% (8.5 to 5.0 cm^{-1}) were found. The scattering power, the relative change of μ_s', was zero in apple, but enhanced in plum over the fruit development period. This mirrors more isotropic and constant structures in apple compared to plum. For horticultural applications, the larger variability in scattering properties of plum explains the discrepancy between commercially assessed NDVI values or similar indices, and the absolute μ_a values in plum ($R < 0.05$), while the NDVI approach appeared reasonable in apple ($R \geq 0.80$).

Abbreviations – DTOF, distribution of time-of-flight; IRF, instrument response function; NDVI, Normalized Differenced Vegetation Index; SNR, signal-to-noise ratio; TRS, time-resolved reflectance spectroscopy; μ_a, absorption coefficient; μ_s', reduced scattering coefficient.

This article has been accepted for publication and undergone full peer review but has not been through the copyediting, typesetting, pagination and proofreading process, which may lead to differences between this version and the Version of Record. Please cite this article as doi: 10.1111/ppl.12232

Introduction

Spectroscopic approach for analyzing optical fruit properties

Fruit represent not only a target for studying general plant developmental processes, but are also of high importance as food source of high nutritional value. Optical properties of fruit are highly relevant for its non-destructive analyses during the whole life cycle of a fruit; and in the agronomic context, e.g. for fruit monitoring in pre- and postharvest processes. Fruit development is characterized by changes in chemical composition (sugar, water, pigment etc. contents) and structural properties (number, size, orientation, and shape of cells, cell walls etc.).

The chemical analyses have been approached non-destructively, by means of spectroscopy in the visible and near infrared (VIS/NIR) wavelength ranges. Simple indices have been established to reduce the impact of scattering in fruits in non-destructive pigment analyses, e.g. on the non-destructive chlorophyll analysis. Frequently, the normalized difference vegetation index (NDVI) was employed, assuming, that the chlorophyll absorption can be measured at 660–690 passband, when correcting for scattering properties measured at 780–810 nm (c.f. Zude 2003). However, this assumption has not been confirmed by deeper analyses of the optical fruit properties. For characterizing the properties of developing fruit, two optical parameters may be used: the absorption coefficient, μa, which provides the absolute number of absorbed photons per cm, and the reduced scattering coefficient, μs', which is the absolute number of scattering events per cm. Generally, two advanced approaches can be used for separating μa and μs': spatial resolved (Peng and Lu 2006, Baranyai and Zude 2009) and time-resolved readings (TRS) (Cubeddu et al. 2001a, Cubeddu et al. 2001b, Kurata et al. 2013). In previous studies significant changes in the fruit optical parameters were measured by TRS in the postharvest period (e.g. in nectarine, plum, and apple) depending on storage conditions (Vanoli et al. 2009, Rizzolo et al. 2010, Lurie et al. 2011, Vangdal et al. 2012). Similarly, we would expect that changes in the optical properties appear during fruit development at the tree.

A basic feature of TRS is that penetration depth is strongly related to the photon time-of-flight. Here, the longer the time-of-flight, the higher the probability for a photon to probe a deeper region. Penetration depth in TRS is therefore influenced by the scattering properties of the probed medium with a required longer time-of-flight for a photon to reach the same depth if the number of scattering events is increased. Interestingly, the absorption coefficient and the source detector distance have no influence on penetration depth, provided the signal-to-noise ratio (SNR) is large enough (Del Bianco et al. 2002). For all these aspects, in the VIS/NIR range TRS is able to probe the tissue of most fruit at a depth of 1–2 cm with available hardware and electronics.

Therefore, when trying to understand the optical fruit properties, we need to consider the fruit morphology in the estimated penetration depth that appears substantially different in fruits. In the present study, the optical properties of stone and pip fruits were exemplarily measured for plum and

apple during growth by means of TRS. The interest in these species is not only related to their wide diffusion in horticulture: Although both fruit tree species, *Prunus domestica* and *Malus x domestica* Borkh., belong to the Rosaceae family, they differ essentially in their fruit forms, and thus their fruit development.

Fruit development and tissue differentiation in plums

Plums represent a one-seeded stone fruit developing from one free carpel not adnated to the cup-like receptacle (Fig. 1a). During fruit development, the ovary tissue differentiates into an inner stony and an outer fleshy pericarp. The fruit growth follows a double-sigmoid curve with three developmental stages after the fruit set.

The development of the fleshy mesocarp starts from isodiametric cells at the pre-bloom stage. In developmental stage I, cell division ceases approximately four weeks after bloom, while cell diameter increases mainly in the second half of the first stage (Sterling 1953). Intercellular spaces increase and mesocarp thickens. During stage II only small enlargement of the mesocarp occurs since mainly the embryo develops (Tukey and Young 1939, Friedrich 1986). The inner epidermis of the ovary hardens into the stony endocarp. In developmental stage III, the “final swell”, cell sizes measured at the maximum diameter increase by approx. 20 times, e.g. from 15 µm to 280 µm in cultivar 'French', or to 312 µm in cultivar 'Imperial' (Sterling 1953). Due to cell elongations in crossing directions, a three-to-four strata differentiation becomes visible in the mesocarp in this phase. Due to the rapid cell enlargement in the central mesocarpic strata, the thickness of the cell wall decreases, the cells are closely compressed, and intercellular spaces become inconspicuous. In total, the fleshy mesocarp comprises of approx. 43 to 48 cell layers. The single row outer epidermis, together with the few rows of the underlying hypodermis, represents the boundary tissue of the pericarp (exocarp) (Tukey and Young 1939, Sterling 1953; Fig. 1a).

Fruit development and tissue differentiation in apple

In contrast to plum, apple represent a pomaceous pseudocarpic fruit with five epigynus drupe-like carpels fused in the middle. Here, the fleshy tissue is mainly formed by the receptacle, a thickened part of the stem (Tukey and Young 1942, Bain and Robertson 1951, Bresinsky et al. 2008; Fig. 1b). The apple fruit increases its size continuously, sigmoidal from bloom to fruit ripening, however, a first growth stage of steeper increase with cell divisions occurring within 21 (Tukey and Young 1942, Bain and Robertson 1951) to 35 (Janssen et al. 2008) or up to 50–60 days (Friedrich et al. 1986) after fertilization. An intermediate stage of retarded fruit growth, like in stone fruit, does not exist.

The inner part of the fleshy tissue, the pith, is separated from the outer cortex by the core line, a region of smaller, tight packed, tangentially elongated cells (Tukey and Young 1942; Fig. 1d). Its position as distance from the skin, i.e., the thickness of the cortex, ranges from 7 mm at 51 days after full bloom in cv. 'Granny Smith' (Bain and Robertson 1951) to 15–19 mm at maturity for different

cultivars (Bain and Robertson 1951, Drazeta et al. 2004, Malladi and Hirst 2010).

In the cortex at the time of bloom a rapid increase both in cell number and cell size starts, with completion of cell division within three weeks, like in the pith tissue. All subsequent increase is by enlargement of both cells and intercellular spaces. Cells in the central cortex region are radially elongated and organized in radial columns with a cell size of about 197 x 340 µm and thin walls (Tukey and Young 1942, Khan and Vincent 1990). The intercellular space in apple tissue increases during fruit growth, reaching up to 20–25% of the volume (Tukey and Young 1942, Reeve 1953, Khan and Vincent 1990, Verboven et al. 2008). The intercellular spaces, like the cells, elongate radially when progressing inwards, and are often larger than the cells (Khan and Vincent 1990, Drazeta et al. 2004, Schotsmans et al. 2004, Verboven et al. 2008). The skin of the fruit is formed by four hypodermal layers of small isodiametric cells and an uniseriate layer of epidermis (Tukey and Young 1942, Verboven et al. 2008).

The aim of this work was (i) to obtain a more comprehensive view on the developmental stages of fruits considering optical properties, and (ii) to explore the impact of the optical properties, in particular the scattering, on the frequently employed approaches for analyzing plum and apple in horticulture.

Materials and methods

Fruit material

Plums cv. 'Tophit plus' budded on 'Wavit', and apples cv. 'Elstar' budded on 'M9' grown in orchards located in Potsdam, Germany, were harvested at four dates (H1–H4): in apple 65 days after full bloom, (dafb), 72 dafb, 121 dafb, and 135 dafb. In plum full bloom occurred ten days earlier than in apples, resulting the harvest days being 75 dafb, 82 dafb, 131 dafb and 145 dafb (Table 1). Fruits were weighted and shipped on the harvest day to Milan, Italy, by plane, stored in cabin luggage. There, time-resolved reflectance spectroscopy (TRS, see below) measurements were performed the day after harvest, approximately after 24 hours at room temperature.

Mechanical properties and chemical data, typically assessed when describing fruit development, were measured for each sample on the second day after harvest, after the fruits were transported in the same way back to Potsdam. Dry and fresh mass and resulting water content was measured. Equatorial diameter of fruit was measured in plum over the lateral cheeks, while in apple the diameter was calculated from the measured circumference, assuming it being circular. As mechanical properties, fruit flesh firmness by means of Magness-Taylor test in apple and the modulus of elasticity in plum were measured (TA.XT.plus Texture Analyser, Winopal Forschungsbedarf GmbH, Germany). Normalized differenced vegetation index (NDVI) values were calculated from remittance spectra measured on the intact fruits as $(I_{780} - I_{660})/ (I_{780} + I_{660})$ (mean of measurements on two sides of each fruit), using a hand-held spectrophotometer (Pigment Analyzer PA1101, CP, Germany). The soluble solids content(SSC) [%Brix] and acidity as malic acid content [%], was wet-chemically determined

for each fruit.

TRS system set-up

The time-resolved reflectance spectroscopy setup used in this study was developed at Politecnico di Milano (Fig. 2). The light source is a fiber laser (SC450-6W, Fianium, UK) providing white-light picosecond pulses, with duration of few tens of picoseconds, adjustable in power by a variable neutral-density attenuator (NT43-770, EdmundOptics, UK). A dichroic mirror (DMLP900, Thorlabs, Germany) is used to cut-off wavelengths longer than 900 nm so as to avoid excess power to reach the investigated sample. A home-made filter wheel loaded with 14 band-pass interference filters (NT-65 series, Edmund Optics, UK) is used for spectral selection in the range of 540–940 nm. A 10× microscope objective (10X Olympus Plan Achromat Objective, 0.25 NA, RMS10X Thorlabs, Germany) is used to couple light in a 100 µm core multimode graded-index fiber (M43L01, Thorlabs, Germany). The fiber is mounted on a 3-axis tilt on a 3-dimensional translational stage (Fiber Launch with FC-Connectorized Fiber Holder, MBT613/M Thorlabs, Germany) for precise alignment. The average power at the distal end of the illuminating fiber is 1 mW. The light remitted by the diffusive sample is detected by 1 mm step index fiber with high numerical aperture (NA = 0.39, M35L01, Thorlabs, Germany). The photon distribution of time-of-flight (DTOF) is measured with a photomultiplier (HPM-100-50, Becker&Hickl, Germany) and a time-correlated single-photon counting board (SPC-130, Becker&Hickl, Germany). A computer controlled shutter (59-253, EdmundOptics, UK) is used to protect the photomultiplier from ambient light when the fibers are not in contact with the sample. The instrument response function (IRF) is obtained facing the injection and the detection fibers, and has a full width at half maximum of about 260 ps (Torricelli et al. 2012). The TRS measurements were performed over the wavelength range of 540 to 940 nm on two opposite sides of each fruit, at 1.5 cm horizontal source-detector distance. Typical acquisition time was 1 s per wavelength.

TRS data analysis

A model for photon diffusion in turbid media was used to analyze TRS data to assess the differentiated optical properties – absorption coefficient, μ_a, and reduced scattering coefficient, μ_s' – of samples (Martelli et al. 2009). To take into account the finite volume of the sample, we have used the model for photon diffusion in a cube with a volume equal to the volume of the measured sample (Taroni et al. 2007). Convolution of the photon diffusion model with the IRF is performed before fitting the experimental data (Cubeddu et al. 1996). To improve the accuracy in the estimate of the optical properties the spectrally constrained fitting approach was used (D'Andrea et al. 2006). An approximation to the Mie theory relates the reduced scattering coefficient to the structural properties of the diffusive sample:

$$\mu_s' = a\left(\frac{\lambda}{\lambda_0}\right)^{-b} \quad \text{(Equation 1)}$$

λ is the wavelength, *a* is the scattering coefficient at wavelength λ_0 = 670 nm, and *b* is a parameter related to the size of scatterers (Mourant et al. 1997, Nilsson et al. 1998). This expression is inserted in the model for photon diffusion, and parameters *a* and *b* are used as fitting parameters. The spectrally constrained fitting methods improve the estimate of both parameters (D'Andrea et al. 2006). In TRS the value of the absorption coefficient affects the estimate of the reduced scattering coefficient. However, the photon diffusion model is valid under the assumption that the absorption coefficient is much lower than the reduced scattering coefficient. This is the case in the range of 730–900 nm that was, consequently used for the model fitting.

TRS performance assessment

System performances were assessed during the whole experiment by means of calibrated solid tissue phantoms – made of epoxy resin, black toner powder with peak absorbance at 900 nm (Fig. 3), and TiO_2 particles (Pifferi et al. 2005). Absorption and reduced scattering spectra were measured of phantoms (A–D) with nominal values at 660 nm of 0.07 cm^{-1} for the absorption coefficient and 5, 10, 15, and 20 cm^{-1} for the reduced scattering coefficient, respectively. The coefficient of variation (CV) was evaluated for the estimate of both the absorption coefficient and the reduced scattering coefficient during longitudinal measurements performed in the period from 5.7. – 14.11.2011.

Statistics

From the TRS measurements, as final values the means were used of the obtained μ_a and μ_s' values from both sides of the fruit. If invalid μ_a values, caused by technical problems during the measurement, occurred in one side, only the value from the other side was used in apple: n = 5 at λ = 670 nm (4 in H1 with one fruit completely excluded, 1 in H2); in plum: n = 15 at λ = 540 nm (7 in H3, 7 in H4 with one fruit completely excluded) and n = 1 at λ = 580 nm (H4). Pearson correlation, Analysis of Variance (ANOVA), and Tukey post-hoc test were run with SPSS statistics version 21.0 (IBM, USA).

Results

Fruit quality

During the 70 days covered by our study, both apple and plum fruits developed as expected with increase in size from H1 to H3, reaching a steady state at H4 (Table 1). Compared to the harvest day, fresh mass in plum was reduced by 2.3–3.7%, with significantly lower weight loss in the first two harvest dates compared to the later ones (ANOVA, $F = 27.6$, $p < 0.001$). In apple, loss in fresh mass was overall lower, ranging between 0.38% and 0.53% in H2–H4, but was comparably high in H1 with

1.2% (ANOVA, F = 97.0, p < 0.001). Fruit flesh firmness in apple and elasticity in plum decreased over the harvest dates, though stronger in the latter when seen as relative values of H1 (Table 1). Water content varied only slightly in apple, but decreased clearly in plum fruits. Further fruit parameters like fresh and dry mass, soluble solids content and malic acid content behaved like expected over time (data not shown). High fruit chlorophyll contents at the harvest days H1 & H2 resulted in a saturated remittance peak around 660 nm, leading to unreliable NDVI values close to 1(Table 1). Thus, only NDVI-values from H3 & H4 could unambiguously be considered. The NDVI values declined strongly in the last two harvest dates in apple, in plum, however, values remained relatively high and even increased again from H3 to H4.

TRS performance

The absorption spectra of four phantoms showed only small difference from the nominal value of 0.07 cm^{-1} at 660 nm with a coefficient of variation (CV) of <1%. The scattering coefficients at 660 nm resembled very well the nominal values of 5, 10, 15 and 20 cm^{-1} with a CV of 2%. These results show the good performance of the TRS system in separating absorbance and reduced scattering coefficients in ranges relevant for the measured fruit samples (Fig. 3). However, the fruit data were calculated for a parallelepiped with equal volume. It can be assumed that when a not curved model solution is used to interpret curved samples, the reduced scattering coefficient can be slightly (i.e. <20%) underestimated.

Fruit optical properties

The absorption spectra in the apple and plum fruit differed in their absolute values but both showed a typical shape with the characteristic peak around 670 nm due to high chlorophyll content in the first two harvest dates H1 and H2 (Fig. 3, left column). As expected, the absorption coefficient showed a decrease at 670 nm during fruit growth in H3 and H4 due to chlorophyll loss. Beyond 800 nm mainly water is assumed to cause slight absorption. In plum, an increased absorption at shorter wavelengths can be referred to the presence of anthocyanins.

More pronounced are the differences in the reduced scattering coefficients for the two fruits (Fig. 3, right column): In apple, the reduced scattering coefficient spectrum is flat at all harvest dates, and much higher than in plums. This is consistent with an equivalent size of scatterers much larger than the wavelength as pointed out in other disciplines (Mourant et al. 1997, Nilsson et al. 1998). Best fitting with Mie were performed with $b = 0$, apparent as zero slope and equivalent to a scattering power value of zero (Fig. 4, upper row). The scattering coefficient at 670 nm, as an interesting wavelength for chlorophyll detection, is significantly declining between the early (H1 & H2) and the late (H3 & H4) harvest dates. However, relative decline of the scattering coefficient reached maximal 14.7% in H4 (compared to H1), indicating a slight reduction in the scattering events in apple.

In plum, in contrast, a significant and stronger decrease in the reduced scattering coefficient was

observed during fruit growth. The scattering coefficient at 670 nm changed significantly from each harvest date to the next one, and reached the maximal reduction of 41.5% in H4 (Fig. 4, lower row, left). Also, the slope of the reduced scattering coefficient, i.e. the parameter *b*, differed significantly between the first and the last two harvest dates (Fig. 4, lower row, right). The value was in H4 by 24.9% lower compared to H1. Thus, the parameter *a* was more affected than the parameter *b* (eq. 1), suggesting a larger change in the density of scatterers rather than in their equivalent size.

Relation between commercially used NDVI and specific optical properties, μ_a & μ_s'

The NDVI is commonly based on the measured intensity value at the passband 660–680 nm normalized by the passband 780–810 nm. Thus, it may be assumed that the above presented absorption coefficient μ_a at 670 nm is related to the NDVI. In the NDVI, however, the (chlorophyll) absorbance signal is not yet separated from the scattering signal, what is the case for the absolute μ_a value.

The NDVI values from the harvest dates H3 and H4 were highly correlated with the μ_a value in apple (H3: $R = 0.90$, $p < 0.001$, $n = 12$; H4: $R = 0.80$, $p = 0.001$, $n = 13$; Fig. 5). In plum, in contrast, no correlation appeared (H3: $R = 0.04$, $p = 0.841$, $n = 36$; H4: $R = –0.04$, $p = 0.874$, $n = 18$). Here, the NDVI values remained over all the developmental stages high, close to the maximum value of 1. The corresponding μ_s' values at 670 nm varied little in apple but stronger in plum (Fig. 4, left column).

Discussion

Fruit tissue measured during the course of fruit growth

The changes in size of developing fruit did not influence the estimate of the optical parameters since the varying fruit volumes were considered in the used photon diffusion model. Given the values of the reduced scattering coefficients (5–20 cm^{-1}) and the average photon time-of-flight (1500–2000 ps) the mean penetration depth for TRS measurement was in the range of 8–16 mm with the smallest values related to the highest scattering. Given the typical thickness of plum exocarp and apple skin (epidermis + hypodermis) is below 1 mm, the measured optical parameters are marginally influenced by the structure and composition of these compartments.

In plum, developmental stage I with predominantly cell divisions, and some growth due to cell enlargement, both in the endocarp and the fleshy mesocarp, is described lasting up to eight weeks after full bloom (Sterling 1953). Following developmental stage II is characterized by stone hardening and retarded fruit growth. Thus, fruits harvest at dates H1 and H2 – dating 11 and 12 weeks after full bloom – with low increase in size (H1: 33.2 mm, H2: 35.2 mm diameter) and non-significant changes in elasticity (Table 1) can be assumed to represent the developmental stage II. Pith size does not continue to increase at this stage, and is reported to lie between 5–13 mm in thickness (Depypere et al. 2007). Thus, the average fruit radius of about 16.6 mm, 17.6 mm, 23.6 mm, and 24.0 mm (Table 1) consisted to approx. 2.5–6.5 mm of the increasingly stony endocarp, and to 10.1–14.1 mm, 11.1–

15.1 mm, 17.1–21.1 mm, and 17.5–21.5 mm of the fleshy mesocarp in H1, H2, H3, and H4, respectively. Since in plum the μs' is in the range of 5–10 cm^{-1} (Fig. 3) and the mean penetration depth is 12–16 mm, the complete mesocarp was measured in all four harvest dates.

In apple, the phase of mainly cell divisions should end latest 50–60 days after fertilization (Friedrich et al. 1986). Thus, our harvest date H1 with 65 dafb should also already represent the growth phase characterized by only cell and intercellular enlargements. Data on the same apple cultivar from the same orchard in the year previous to our study revealed the position of the core line as distance from the skin, i.e. the thickness of the cortex, between 12.0 to 18.8 mm (mean 15.3 mm) in apple corresponding in size to those of H2 already, and between 17.4 to 23.2 mm (mean 19.9 mm) to those of H3. The distance between the skin and the outermost point of the pericarp (Fig. 1d) was between 15.5 to 20.8 mm (mean 18.3 mm) in the H2-sized fruits, and between 23.5 to 30.6 mm (mean 26.8 mm) in the H3 equivalents. In apple the changes in the reduced scattering coefficient were in the range of 15–20 cm^{-1}, and therefore mean penetration depth varies in the range of 8–10 mm Thus, light should have penetrated only the relatively isotropic cortex tissue at all four harvest dates.

Relation of optical measurements to fruit tissue structure

Variance in the optical properties of both apple and plum were found in fruit harvested at the same date. This was an expected result, since there is a natural biological variability considering the phenotypical appearance (Fig. 3). Moreover, differences in the optical properties were also observed among different harvest dates. As expected these differences are more pronounced between early and late harvest, when fruit changes due to development are more evident (see also mechanical properties, Table 1). In apple however, these optical changes appear relatively smaller than in plum (Fig. 4, left column), since in apple only the cell size and intercellular space increased. In plum, during the final swell at the time of the late harvest dates H3 & H4, cells enlarge in different directions depending on the three to four strata, and here cells get increasingly closely compressed resulting in reduced intercellular space. The structural change probably most relevant for the changes in the optical (in particular scattering) signal is the decrease in cell wall thickness, what was paralleled by the strong decline in the elastic modulus of plum (down to 23% compared to H1, Table 1).

By means of the scattering power and the scattering coefficient at 670 nm (Fig. 4) it can be pointed out that the variation in apple is much lower compared to the variation over fruit growth in plum fruit. This has a practical consequence, when using non-destructive sensors for classical spectroscopy (Merzlyak et al. 1999), which provide the sum signal of μ_s' and μ_a (Fig. 5). Calibrations on the chlorophyll content are stable over the period of fruit development in apples (Zude 2003). However, perturbations can be expected in plum. In *Prunus avium*, also stone fruit, it was shown that the calibration on pigment contents (anthocyanins) were stable, only when a reasonable correction was carried out considering the varying scattering properties (Zude et al. 2011). From the present data such findings were confirmed for plum.

Absolute values of scattering events were higher in apple in comparison to plum (Fig. 3) what is assumed to be due to more scatterers in apple. From the scattering power we can derive that, in plum, the size of the scatterers is more related to smaller wavelengths than to larger ones, while in apple over the measured range no response to the changing wavelength was found (Fig. 4).

Conclusions

In the present study, the photons penetrated the fleshy part of the fruits with almost no influence of the skin both in apple and plum. Reasonable absorption spectra related to chlorophyll were calculated for both fruits. The reduced scattering coefficients were characterized over the course of fruit growth, pointing to (i) smaller scatterer size in plum compared to apple, and (ii) "stable" cortex tissue in apple and highly variable tissue in plum in the developmental stages II and III. The NDVI was confirmed to show a high correlation with the absolute absorption coefficient at 670 nm in apple. In plum, it has been shown that the sum signal measured is not correlated with the absolute absorption coefficient. The variation in the scattering properties was pointed out as the perturbation on the non-destructive reading. Consequently, corrections are required considering the scattering properties of the fruit.

Author contributions

Birgit Seifert performed the literature search, the statistical analyses, writing of introduction and parts of the discussion. She developed all figures and tables by getting a red line into the presentation.
Manuela Zude provided the hypothesis assuming that NDVI is not stable in stone fruit, while – to own experiences – it will be stable in apple. Manuela had the idea that the scattering coefficient might be the cause for such perturbations. She set-up the experimental design and supervised the work of Mrs Seifert. The text on the results and parts of the discussion was mainly written by her. Lorenzo Spinelli performed the TRS readings and developed software for the data analyses according to Mie theory. Alessandro Torricelli set-up the TRS measures and carried out the data analyses. He provided the text on the material and methods as well as the background on TRS.

Acknowledgements – Research has been carried out in the framework of the USER-PA Project (FP7, ICT-AGRI), targeting the USability of Environmentally sound and Reliable techniques in Precision Agriculture, and LASERLAB-EUROPE (FP7-INFRASTRUCTURES-2011-1, INFRA-2011-1.1.19. Laser sources, Grant agreement no: 284464). We are grateful to the editor of the Journal of the Torrey Botanical Society for granting copy right permission for Fig. 1c.

References

Bain JM, Robertson RN (1951) The physiology of growth in apple fruits. 1. Cell size, cell number, and fruit development. Aust J Sci Res B-Biol Sci 4: 75–91

Baranyai L, Zude M (2009) Analysis of grades and bruising of kiwifruit using laser-induced backscattering imaging. Computers and Electronics in Agriculture 69: 33–39

Bresinsky A, Körner C, Kadereit J, Neuhaus G, Sonnewald U (2008) Strasburger Lehrbuch der Botanik, 36th edition. Spektrum Akademischer Verlag, Heidelberg

Cubeddu R, Pifferi A, Taroni P, Torricelli A, Valentini G (1996) Experimental test of theoretical models for time-resolved reflectance. Medical Physics 23: 1625–1633

Cubeddu R, D'Andrea C, Pifferi A, Taroni P, Torricelli A, Valentini G, Ruiz-Altisent M, Valero C, Ortiz C, Dover C, Johnson D (2001a) Time-resolved reflectance spectroscopy applied to the non-destructive monitoring of the internal optical properties in apples. Appl Spectrosc 55: 1368–1374

Cubeddu R, D'Andrea C, Pifferi A, Taroni P, Torricelli A, Valentini G, Dover C, Johnson D, Ruiz-Altisent M, Valero C (2001b) Non-destructive quantification of chemical and physical properties of fruits by time-resolved reflectance spectroscopy in the wavelength range 650–1000 nm. Appl Opt 40: 538–543

D'Andrea C, Spinelli L, Bassi A, Giusto A, Contini D, Swartling J, Torricelli A, Cubeddu R (2006) Time-resolved spectrally constrained method for the quantification of chromophore concentrations and scattering parameters in diffusing media. Op Express 14: 1888–1898

Del Bianco S, Martelli F, Zaccanti G (2002) Penetration depth of light re-emitted by a diffusive medium: theoretical and experimental investigation. Phys Med Biol 47: 4131–4144

Depypere L, Chaerle P, Mijnsbrugge KV, Goetghebeur P (2007) Stony endocarp dimension and shape variation in *Prunus* section *Prunus*. Ann Bot 100: 1585–1597

Drazeta L, Lang A, Hall AJ, Volz RK, Jameson PE (2004) Air volume measurement of 'Braeburn' apple fruit. J Exp Bot 55: 1061–1069

Friedrich G, Neumann D, Vogl M (1986) Physiologie der Obstgehölze, 2th edition. Akademie-Verlag, Berlin

IBM Corp (2010) IBM SPSS Statistics for Windows, Version 19.0. IBM Corp., Armonk, NY, USA

Janssen B, Thodey K, Schaffer R, Alba R, Balakrishnan L, Bishop R, Bowen J, Crowhurst R, Gleave A, Ledger S, McArtney S, Pichler F, Snowden K, Ward S (2008) Global gene expression analysis of apple fruit development from the floral bud to ripe fruit. BMC Plant Biol 8: 16

Khan AA, Vincent JFV (1990) Anisotropy of apple parenchyma. J Sci Food Agric 52: 455–466

Kurata Y, Tsuchida T, Tsuchikawa S (2013) Time-of-flight near-infrared spectroscopy for nondestructive measurement of internal quality in grapefruit. J Am Soc Hort Sci 138: 225–228

Lammertyn J, Peirs A, De Baerdemaeker J, Nicolaı B M (2000) Light penetration properties of NIR radiation in fruit with respect to non-destructive quality assessment. Postharvest Biol Technol 18: 121–132

Lurie S, Vanoli M, Dagar A, Weksler A, Lovati F, Eccher Zerbini P, Spinelli L, Torricelli A, Feng J, Rizzolo A (2011) Chilling injury in stored nectarines and its detection by time-resolved reflectance spectroscopy. Postharvest Biol Technol 59: 211–218

Malladi A, Hirst PM (2010) Increase in fruit size of a spontaneous mutant of 'Gala' apple (*Malus* x *domestica* Borkh.) is facilitated by altered cell production and enhanced cell size. J Exp Bot 61: 3003–3013

Martelli F, Del Bianco S, Ismaelli A, Zaccanti G (2009) Light Propagation through Biological Tissue and Other Diffusive Media: Theory, Solutions, and Software. SPIE Press, Washington, USA

Merzlyak MN, Gitelson AA, Chivkunova OB, Rakitin VY (1999) Non-destructive optical detection of pigment changes during leaf senescence and fruit ripening. Physiol Plant 106: 135–141

Mourant J R, Fuselier T, Boyer J, Johnson TM, Bigio IJ (1997) Predictions and measurements of scattering and absorption over broad wavelength ranges in tissue phantoms. Appl Opt 36: 949–957

Nilsson AMK, Sturesson C, Liu DL, Andersson-Engels S (1998) Changes in spectral shape of tissue optical properties in conjunction with laser-induced thermotherapy. Appl Opt 37: 1256–1267

Peng, YK, Lu RF (2006) Improving apple fruit firmness predictions by effective correction of multispectral scattering images. Postharvest Biol Technol 41: 266–274

Pifferi A, Torricelli A, Bassi A, Taroni P, Cubeddu R, Wabnitz H, Grosenick D, Möller M, MacDonald R, Swartling J, Svensson T, Andersson-Engels S, van Veen RLP, Sterenborg HJCM, Tualle J, Nghiem HL, Avrillier S, Whelan M, Stamm H (2005) Performance assessment of photon migration instruments: the MEDPHOT protocol. Appl Opt 44: 2104–2114

Reeve RM (1953) Histological investigations of texture in apples. J Food Sci 18: 604–617

Rizzolo A, Vanoli M, Spinelli L, Torricelli A (2010) Sensory characteristics, quality and optical properties measured by time-resolved reflectance spectroscopy in stored apples. Postharvest Biol Technol 58: 1–12

Ruiz-Altisent M, Ruiz-Garcia L, Moreda GP, Lu RF, Hernandez-Sanchez N, Correa EC, Diezma B, Nicolaï B, García-Ramos J (2010) Sensors for product characterization and quality of specialty crops – A review. Computers and Electronics in Agriculture 74: 176–194

Saeys W, Velazco-Roa MA, Thennadil SN, Ramon H, Nicolaï BM (2008) Optical properties of apple skin and flesh in the wavelength range from 350 to 2200 nm. Appl Opt 47: 908–919

Schotsmans W, Verlinden BE, Lammertyn J, Nicolai BM (2004) The relationship between gas transport properties and the histology of apple. J Sci Food Agric 84: 1131–1140

Spinelli L, Rizzolo A, Vanoli M, Grassi M, Eccher Zerbini P, Meirelles de Azevedo Pimentel R, Torricelli A (2012) Optical properties of pulp and skin in Brazilian mangoes in the 540–900 nm spectral range: implication for non-destructive maturity assessment by time-resolved reflectance spectroscopy. International Conference of Agricultural Engineering, CIGR-Ageng2012, July 8–12, Valencia, Spain, paper C2096

Sterling C (1953) Developmental anatomy of the fruit of *Prunus domestica* L. Bulletin of the Torrey Botanical Club 80: 457–477

Taroni P, Comelli D, Farina A, Pifferi A, Kienle A (2007) Time-resolved diffuse optical spectroscopy

of small tissue samples. Opt Express 15: 3301–3311

Tukey HB, Young JO (1939) Histological Study of the Developing Fruit of the Sour Cherry. Bot Gaz 100: 723–749

Tukey HB, Young JO (1942) Gross Morphology and Histology of Developing Fruit of the Apple. Bot Gaz 104: 3–25

Vangdal E., Eccher Zerbini P, Vanoli M, Rizzolo A, Lovati F, Torricelli A, Spinelli L (2012) Detecting internal physiological disorders in stored plums (*Prunus domestica* L.) by time-resolved reflectance spectroscopy. Acta Hortic 945: 197–204

Vanoli M, Eccher Zerbini P, Spinelli L, Torricelli A, Rizzolo A (2009) Polyuronide content and correlation to optical properties measured by time-resolved reflectance spectroscopy in 'Jonagored' apples stored in normal and controlled atmosphere. Food Chem 115: 1450–1457

Verboven P, Kerckhofs G, Mebatsion HK, Ho QT, Temst K, Wevers M, Cloetens P, Nicolaï BM (2008) Three-Dimensional Gas Exchange Pathways in Pome Fruit Characterized by Synchrotron X-Ray Computed Tomography. Plant Physiol 147: 518–527

Zude M (2003) Comparison of indices and multivariate models to non-destructively predict the fruit chlorophyll by means of visible spectrometry in apples. Anal Chim Acta 481: 119–126

Zude M, Pflanz M, Spinelli L, Dosche C, Torricelli A (2011) Non-destructive analysis of anthocyanins in cherries by means of Lambert-Beer and multivariate regression based on spectroscopy and scatter correction using time-resolved analysis. J Food Eng 103: 68–75

Edited by S. Pelaz

Figure legends

Fig. 1. Upper row: Drawings demonstrating basic flower parts (i.e., – sepal (s), st – stamen (st), and carpel; petals were left out for clarity), and differences among flowers of *Prunus* (a) and *Malus* (b) species. Lower row: Cross-sections of corresponding fruits: (c) plum (cv. 'French', two weeks after full bloom; changed after Sterling 1953, with permission of the Journal of the Torrey Botanical Society), and (d) apple fruit (cv. 'Elstar', approximately 16 weeks after full bloom in 2010 (19.08.2010); stained with Lugol's solution).

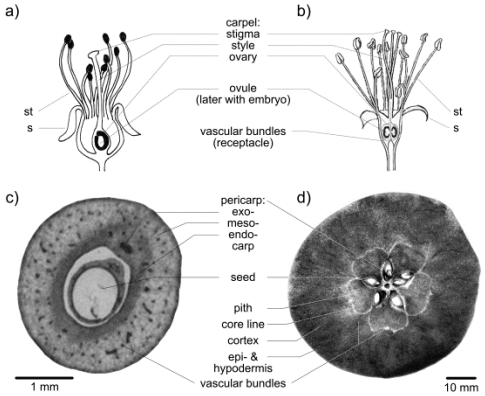

Fig. 2. Scheme of the system set-up for time-resolved reflectance spectroscopy. TCSPC: time-correlated single photon counting.

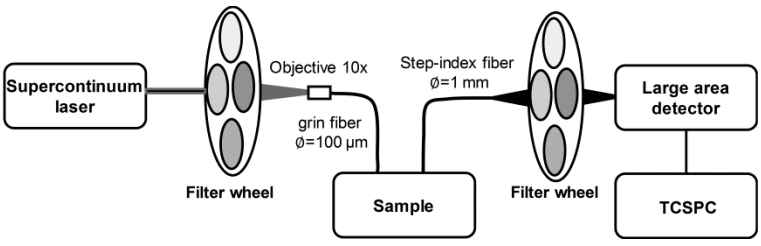

Fig. 3. Absorption (μ_a, left) and reduced scattering (μ_s', right) spectra of phantoms A–D (upper row) combining fixed μ_a-values with varying μ_s'-values (as example measurements at H4, other dates were very similar), and of apple and plum samples (lower two rows) from the four harvest dates H1–H4. The continuous lines in the right graphs are the best fit of the reduced scattering spectrum with the Mie approximation. Bars represent mean ± 1 standard deviation.

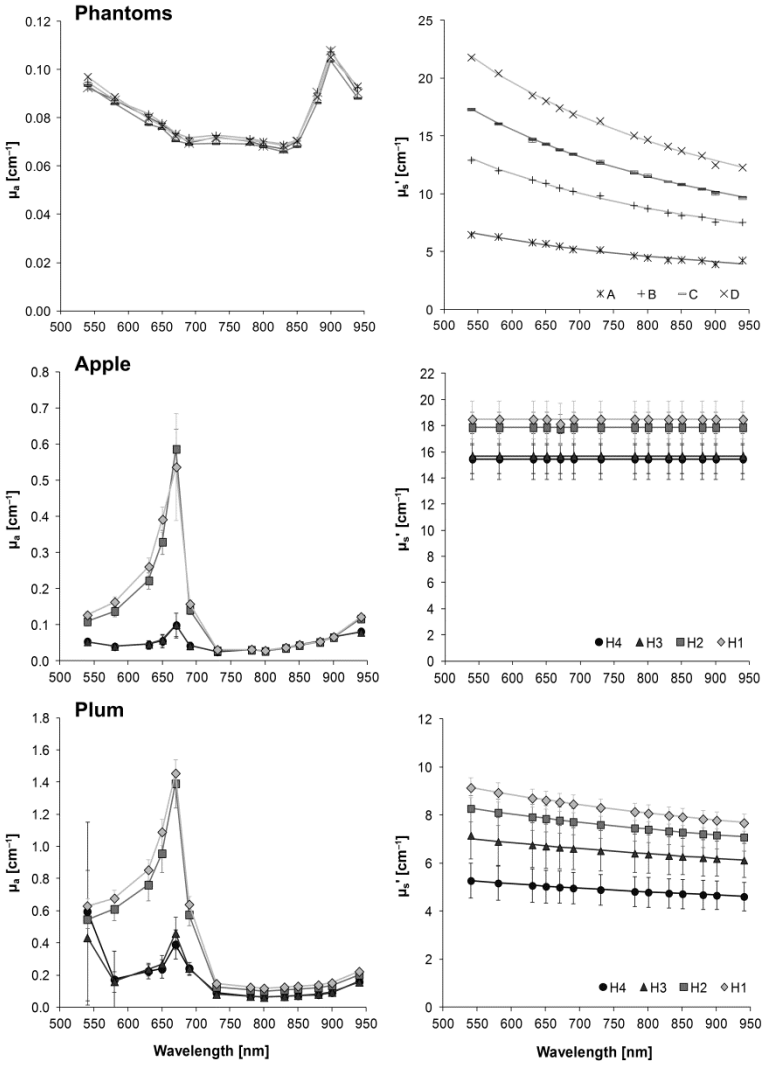

Fig. 4. Reduced scattering coefficient μ_s' at 670 nm (i.e., parameter *a*) as relative value in relation to the mean value of the first harvest date (=100%; left column), and scattering power *b* (right column) for apple and plum. Bars represent mean ± 1 standard error. Different letters each represent significant differences among the fruit development stages (one-way ANOVA with Tukey post-hoc test) as characterized by number of days after full bloom (dafb). For μ_s' at 670 nm (left column) the ANOVA refers to the absolute values (presented in Fig. 3).

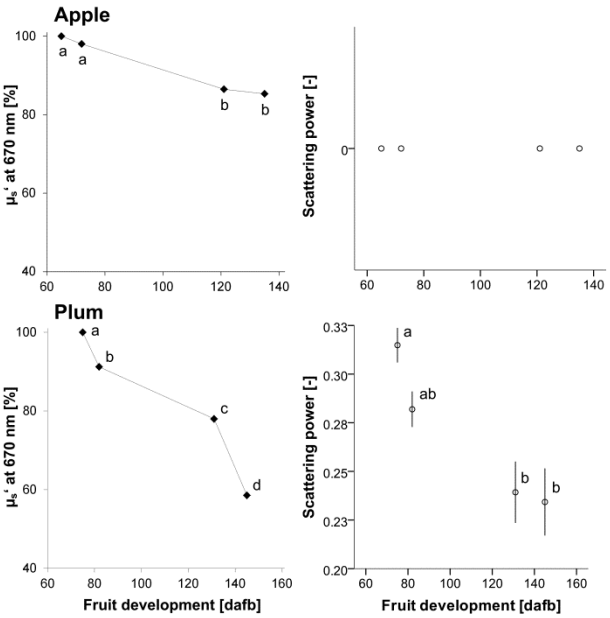

Fig. 5. Correlation between averaged absorption coefficient μ_a at 670 nm for the late harvest dates H3 (triangle) and H4 (circle) and the corresponding NDVI values in apple and plum fruit. Data from H1 & H2 could not be evaluated for technical reasons.

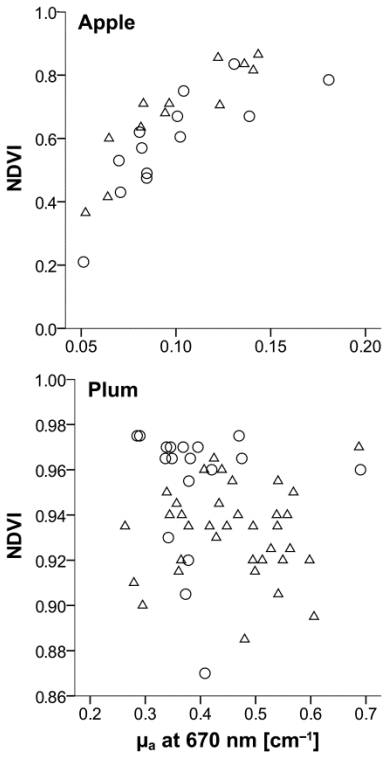

Tables

Table 1: Number, fruit development (days after full bloom, dafb), size, mechanical properties, water content and NDVI (normalized difference vegetation index) value (mean ± standard deviation) of apple (n_{total} = 53) and plum (n_{total} = 117) fruits at the four harvest dates H1 to H4 in the year 2011. Different letters indicate significant differences among the harvest dates within each variable; the according F-values are given (ANOVA with Tukey post-hoc test).

Harvest date	**H1 (04/07)**	**H2 (11/07)**	**H3 (29/08)**	**H4 (12/09)**	**F-value***
Apple					
Number	13	15	12	13	
Fruit development [dafb]	65	72	121	135	
Diameter [mm]	53.2 ± 2.8^{a}	57.6 ± 3.1^{a}	76.8 ± 8.6^{b}	74.6 ± 3.7^{b}	73.8
Firmness [N]	116.5 ± 5.7^{a} (100%)	109.7 ± 9.9^{a} (94.2%)	69.6 ± 7.5^{b} (59.7%)	65.4 ± 4.6^{b} (56.2%)	172.4
Water content [%]**	83.3 ± 0.8^{a}	84.8 ± 0.8^{b}	83.8 ± 1.4^{ab}	84.0 ± 1.1^{ab}	5.1
NDVI [0;1]	0.97 ± 0.00^{a}	0.97 ± 0.00^{a}	0.68 ± 0.16^{b}	0.59 ± 0.17^{b}	40.7
Plum					
Number	32	31	36	18	
Fruit development [dafb]	75	82	131	145	
Diameter [mm]	33.2 ± 1.6^{a}	35.3 ± 2.1^{b}	47.2 ± 2.3^{c}	47.9 ± 3.3^{c}	334.5
Elasticity modulus [N/cm²]	4.4 ± 0.6^{a} (100%)	4.6 ± 0.6^{a} (106.4%)	1.8 ± 0.6^{b} (40.7%)	1.0 ± 0.4^{c} (22.7%)	290.1
Water content [%]	84.4 ± 0.6^{a}	86.8 ± 1.2^{b}	78.7 ± 1.7^{c}	67.6 ± 5.0^{d}	308.4
NDVI [0;1]	0.97 ± 0.01^{a}	0.97 ± 0.01^{a}	0.93 ± 0.02^{b}	0.95 ± 0.03^{c}	41.3

* Degrees of freedom: Apple: df1 = 3, df2 = 49; Plum: df1 = 3, df2 = 113; p-value for all: < 0.001, except water content in apple: p = 0.004.
** Water content in apple for H1 might be underestimated compared to H2-H4 due to varying (transport) conditions, see methods for further details.